

## Article

# Multi-Analytical Assessment of Bodied Drying Oil Varnishes and Their Use as Binders in Armour Paints

Francesca Caterina Izzo <sup>1</sup>, Arja Källbom <sup>2,\*</sup> and Austin Nevin <sup>3</sup>

<sup>1</sup> Sciences and Technologies for the Conservation of Cultural Heritage, Department of Environmental Sciences, Informatics and Statistics, Ca' Foscari University of Venice, Via Torino 155/b, 30173 Venice, Italy; fra.izzo@unive.it

<sup>2</sup> Department of Conservation, University of Gothenburg, 40530 Gothenburg, Sweden

<sup>3</sup> Courtauld Institute of Art, Somerset House, London WC2R 0RN, UK; austin.nevin@courtauld.ac.uk

\* Correspondence: arja.kallbom@conservation.gu.se

**Abstract:** The characteristics of commercially available refined and bodied linseed and tung oils, used as binders in the production of armour paints after historic recipes, are explored. Employed as anticorrosive paints mainly from the 1920s to 1960s, armour paints are greener alternatives that can be used for protection in industrial heritage conservation. Using a multi-analytical approach, chemical and physical properties of the fresh oils and solid films before and after accelerated ageing (ISO 16474-2:2013) were investigated to better understand which features are beneficial for the technical function of armour paints. Tests included measurements of density, the refractive index, insoluble impurities, alkaline impurities, the water content, the iodine value, the saponification value, the free fatty acid concentration, the acid value, the peroxide value and colour (Lovibond) and cold tests. The characterisation of the fresh oils using molecular analysis with FTIR and GC-MS revealed the complexity of the commercial formulations, for which additions of semi- and non-drying oils were detected. The results show that organic paint binders follow complex chemical reactions (such as oxidation and decrease of unsaturation being variable or swelling following water-immersion tests), with implications for their suitability for use in protection.

**Keywords:** armour paints; bodied drying oils; anticorrosive coating; ferrous heritage; stand oil; tung oil; air-blown varnish; modern linseed oil; drying oil oxidation; ageing; imbibition



check for updates

**Citation:** Izzo, F.C.; Källbom, A.; Nevin, A. Multi-Analytical Assessment of Bodied Drying Oil Varnishes and Their Use as Binders in Armour Paints. *Heritage* **2021**, *4*, 3402–3420. <https://doi.org/10.3390/heritage4040189>

Academic Editor: Nicola Masini

Received: 20 August 2021

Accepted: 12 October 2021

Published: 14 October 2021

**Publisher's Note:** MDPI stays neutral with regard to jurisdictional claims in published maps and institutional affiliations.



**Copyright:** © 2021 by the authors. Licensee MDPI, Basel, Switzerland. This article is an open access article distributed under the terms and conditions of the Creative Commons Attribution (CC BY) license (<https://creativecommons.org/licenses/by/4.0/>).

## 1. Introduction

This work aims to investigate the ageing characteristics of binders alone in order to reveal more information about their function as part of armour paints. Armour paints are paint systems that have shown remarkable performance and have lasted outdoors for over 85 years, as exemplified by the Oat Mill in Stockholm [1]. The concept and ageing characteristics of aluminium-pigmented armour paint—a historical, anticorrosive paint type from the early 20th century—entail excellent protection for weather-exposed ferrous substrates [1,2]. Armour paints are of particular relevance for historical ferrous objects for which there is a need for sustainable and greener paint systems and a desire to replicate historical practices in applications. In its original concept, armour paint is applied to ferrous surfaces and consists of two layers of a primer of red-lead linseed oil paint and two layers of lamellar specularite and leafing aluminium pigments bound in bodied linseed and a tung stand oil mixture (i.e., drying oil varnishes). With ageing, historical and replica paints (based on historical recipes) become highly oxidised, but natural ageing for four years in southern Sweden and accelerated ageing (according to ISO 16474-2:2013) were found to result in approximately equal ageing characteristics, and a high proportion of unsaturated fatty acids remained in the sub-surfaces of the replica paints [2].

The motivation for assessing binders in this work is that there has been a confusing debate in Sweden among stakeholders, heritage agencies, producers and master painters

about how to make and use linseed oil paints for the protection of outdoor heritage objects. Oil varnishes have been used as binders for paint-making for centuries but, after the Second World War, they were outcompeted by other paint types, such as alkyds and paint with a petrochemical origin [3]. Until about 1890, linseed oxide varnishes were commonly produced by adding driers of metal oxides (such as lead and/or manganese), which were dissolved by high-temperature heat treatments of the purified oil [3,4]. This method continued to be used until ca. 1920. In ca. 1890, a new procedure was introduced where liquid driers (different lead, manganese and cobalt compounds) were dissolved in resins, drying oils, fatty acids or naphthenes and added to the oils at a substantially lower temperature, which also led to different characteristics in the solid films (compared to the oxide varnishes). Later in the 20th century, other types of liquid driers were introduced.

For anticorrosive paints, fat oil varnishes—such as heat-bodied oxide varnishes, stand oils and linseed oils added to tung oil mixtures—have been used as binders since they improve the paint layers' impermeability and hydrophilicity (these are important features of weather-exposed paints in order to resist initiation of under-film corrosion) [4]. For anticorrosive paints, cold-pressed and purified linseed oils are recommended as they are believed to produce high-quality films [5,6]. Raw linseed oils, or boiled linseed without any addition of driers, should never be used for the same reasons. In Sweden and elsewhere, the production of linseed oils and paints was resumed in the 1990s but not on a scale comparable to historical periods. Most contemporary linseed oil paints in Sweden use cold-pressed linseed oils, heated to 120–150 °C and air-blown, with liquid driers, such as Co-Zr ethyl hexanoate/octanoate/propionate.

The characteristics and ageing of drying oil and varnishes are most often described in terms of oxidation, polymerisation and hydrolysis [7,8]. Until the mid-20th century, it was common for technical descriptions to also consider the colloidal state of the oils and varnishes [4,9,10]. This is an aspect that has been recognized in conservation science, with Dietemann stating that the colloidal aspects of the paint are often “forgotten, overlooked, or ignored” [11]. The colloidal state of the oil or varnish is determined by factors such as purification treatments, heat treatments and the type of drier [4]. The colloidal nature of the solid film (or gel) affects its characteristics, such as its solubility in different solvents. This is relevant for exterior paints since environmental water and moisture are polar solvents.

The investigation of binders in this work was based on an analysis of the different chemical and physical characteristics of binders and films to reveal differences in compositions and responses to accelerated ageing conditions. FTIR spectroscopy and GC-MS analysis were conducted on unaged liquid and solid varnishes and aged solid films to probe the chemical modifications that occur with ageing of the paint binders. Different laboratory methods were used for the assessment of chemical and physical bulk properties to find out if any correlation could be identified between the chemical composition and the performance of the oils as binders. The physical properties of oil films were tested using a glass-plate method, used by varnish producers in the 1930s, specifically to assess the resistance to water exposure for solid varnishes. For comparison, two other varnishes were studied: a litharge varnish was added, as this type was used historically until the 1920s [3], and pyrolusite and manganese borate varnishes were tested, since the oxide varnishes were used for demanding applications and heat-bodied at higher temperatures than the modern linseed oil varnishes.

## 2. Materials and Methods

### 2.1. Materials and Sample Overview

The following commercially available drying oils were investigated to compare the influence of air blowing, heat bodying and the presence of stand oil in paints: (1) a modern, air-blown linseed oil varnish (OH), (2) a heat-bodied manganese oxide varnish (WHT), (3) a linseed stand oil with a viscosity of 50 dPa·s (WS) and (4) a mixture of (2) + 20 wt% bodied tung oil (WT). Details of the binders can be found in supplement A in [2]. Additional binders were also assessed using water immersion tests and included an oil boiled at

high temperature with litharge addition (L), pyrolusite varnish (P) and a manganese borate varnish (MB). The variants were analysed in liquid and solid form; i.e., as fresh and (partially) dried paint mixtures. The solid state was investigated in unaged reference samples and at two points during artificial ageing, as outlined in Table 1.

**Table 1.** Overview of the oil binders studied. Each oil was studied at equivalent exposures corresponding to four weeks following application, with 64 kJ and 97 kJ exposure to filtered Xenon light as part of ISO 16474-2:2013 cyclical testing.

Typology (Drying Oil Used)	Paint Name	Description	Exposure
OH Air-blown linseed oil varnish (heated to 130–150 °C, drier: Co-Zr ethyl hexane/octate/proprionate).	OH-L	Liquid	Fresh oil
	OH-0	Solid film—unaged	4 weeks naturally aged
	OH-A1	Solid film—aged 1	64 kJ
	OH-A2	Solid film—aged 2	97 kJ
WHT Heat-bodied manganese compound varnish (boiled at high temperature, 280 °C).	WHT-L	Liquid	Fresh oil
	WHT-0	Solid film—unaged	
	WHT-A1	Solid film—aged 1	64 kJ
	WHT-A2	Solid film—aged 2	97 kJ
WS Stand oil—linseed stand oil, 50 dPa·s	WS-L	Liquid	Fresh oil
	WS-0	Solid film—unaged	
	WS-A1	Solid film—aged 1	64 kJ
	WS-A2	Solid film—aged 2	97 kJ
WT 80 wt% WHT + 20 wt% bodied tung oil	WT-L	Liquid	Fresh oil
	WT-0	Solid film—unaged	
	WT-A1	Solid film—aged 1	64 kJ
	WT-A2	Solid film—aged 2	97 kJ
T Bodied tung oil	T	Liquid	For chemical and physical quantification only
L	L-0	Unaged	Litharge varnish *
P	P-0	Unaged	Pyrolusite varnish *
MB	MB-0	Unaged	Manganese borate varnish *
OHT	OHT-0	Unaged	OH with 20 wt% tung oil *

\* Water immersion test only.

#### Application of Liquid Oils and Varnishes to Steel Sheet Substrate

Mild steel sheets, commonly used for steel-sheet roofing (Dogal DC10 from SSAB), with a size of 75 × 95 mm were coated with oil binders. The chemical composition of the steel was C 0.12 wt%, Mn max 0.8 wt% and P and S max 0.045 wt%. The steel sheets were degreased with ethanol, rubbed with fine steel wool and detergent to a surface profile of  $Ra\ 6 \pm 1\ \mu\text{m}$ , washed in water and dried. Immediately before coating, the surfaces were washed and wiped off in ethanol and air dried. The coating was applied with a drawdown bar. The thickness of the solid film was  $18\text{--}22\ \mu\text{m} \pm 3\ \mu\text{m}$  and was measured by a magnetic, inductive, handheld Permascope device (25 measurements per sample). The films were dried at room temperature, RH 37–40%, for four weeks prior to accelerated ageing. The effects of autophobicity as described in [12] were observed mainly for OH, but films that appeared to be satisfyingly smooth, dense and without apparent defects visible in daylight and UV light were chosen for the accelerated ageing. The solid films were, despite this, expected to contain some inhomogeneities. When the binder is mixed with pigment, the effects of the autophobicity of the air-blown varnish (OH) are less pronounced, as described in previous work [1,2].

## 2.2. Ageing Conditions

Accelerated ageing was carried out in a climate chamber by using a standardised cyclic test [13], the Xenotest 440 from Atlas Instruments. The samples were exposed to controlled cyclic humidity and UV light (Xenon arc lamps with a wavelength distribution similar to daylight). Three samples of each variant were placed in the climate chamber and removed in intervals until the test was stopped after 27 h. The degradation of organic films (without pigments) appeared to be very rapid. A preliminary test series revealed that the solid varnish films were heavily deteriorated and had practically disappeared from the substrate during the exposure of two weeks. Therefore, a much shorter regime was chosen to examine the rapid changes that occur in the initial stages of oxidation: the first aged sample (A1) of each variant was removed after 17 h and the second (A2) after 27 h (and they were not put back into the chamber after the removals). All aged samples showed rusty areas, indicating that moisture had already reached the steel/varnish interface. It could also be observed that the films were partly absent, i.e., the ageing had eroded films from the substrate.

## 2.3. Investigations and Analytical Methods

### 2.3.1. Testing Chemical and Physical Properties of the Oils

The following chemical and physical properties were assessed by a quality-certified oil laboratory according to common procedures and standards: density, refractive index, cold test, insoluble impurities, alkaline impurities, water content, iodine value, saponification value, free fatty acids, acid value, peroxide value and colour (Lovibond).

Appendix A lists the specific methodologies/standards adopted for each measured property/characteristic. The measurements were assessed with a relative Sd of a maximum of 0.5%, and blank and control references are used.

### 2.3.2. Fourier-Transform Infrared Spectroscopy

Analysis of liquid and (unaged and aged) solid films was carried out by Fourier-transform infrared spectroscopy (FTIR). A Bruker Optics Alpha FTIR spectrometer was used in attenuated (ATR) mode with a diamond cell. The spectrometer was equipped with a Pt/SiC globar source, a RockSolid interferometer (with gold mirrors) and a deuterated triglycine sulphate (DLATGS) detector, operating at room temperature and giving a linear response in the spectral range between 7500 and 375  $\text{cm}^{-1}$ . Measurements in ATR mode of liquids and micro-samples from the surface were analysed with a resolution of 4  $\text{cm}^{-1}$  and 128 scans.

### 2.3.3. Gas Chromatography–Mass Spectrometry

To fully characterise the organic lipidic fraction and better understand the effect of the ageing conditions on the paint mixtures, GC-MS was applied on both liquid oils and (unaged and aged) solid films. Following a GC-MS procedure already tested on modern lipidic mixtures [14–21], small samples of oil films (weights ranging from 0.10 to 0.20 mg) were treated with 50  $\mu\text{L}$  of *m*-(trifluoromethylphenyl)trimethylammonium hydroxide with 2.5% methanol in an overnight reaction at room temperature. One microlitre of the obtained derivatised solution was automatically injected by an AS1310 autosampler (Thermoscientific, Waltham, MA, USA) in a Trace GC 1300 system-equipped ISQ 7000 MS with a quadrupole analyser (Thermoscientific). The chromatographic separation was performed on a chemically bonded, fused silica capillary DB-5MS Column (30 m length, 0.25 mm, 0.25  $\mu\text{m}$ —5% phenyl methyl polysiloxane), using helium as the carrier gas (1 mL/min flow rate). The inlet temperature was 280  $^{\circ}\text{C}$ , and the MS interface was at 280  $^{\circ}\text{C}$ . The transfer line was at 280  $^{\circ}\text{C}$  and the MS source temperature was 300  $^{\circ}\text{C}$ . The temperature was programmed from 50  $^{\circ}\text{C}$  (held for 3 min) to 320  $^{\circ}\text{C}$  (held for 5 min), with a ramp of 10  $^{\circ}\text{C}/\text{min}$ . The MS scans were performed in full-scan mode, considering the range from 40 to 650  $m/z$ , with 1.9 scans/s. The electron ionisation energy was 70 eV. The compounds were identified as methyl ester (following a transesterification reaction) by comparison

with the NIST and MS Search 1.7 libraries of mass spectra and a library created by the authors. Quantitative analysis was undertaken using nonadecanoic acid as the internal standard and a standard solution containing saturated (myristic, palmitic, stearic, azelaic, suberic and sebacic) and unsaturated (oleic, linoleic, linolenic and palmitoleic) fatty acids and glycerol.

The most significant molar ratios among the fatty acids considered in this study were: P/S (palmitic to stearic acid ratio), which is commonly used to suggest the type of drying oil; A/P (azelaic to palmitic acid ratio), D/P (ratio of the sum of the dicarboxylic acids—azelaic, suberic, sebacic and pimelic—to palmitic acid) and D% (total percentage of dicarboxylic acids – azelaic + suberic + sebacic + pimelic), used to provide information on the degree of oxidation of oil; and, finally, the O/S ratio (oleic to stearic acid ratio), which can indicate the maturity of oils [14].

#### 2.3.4. Water Immersion Test

The test used for the water absorption and imbibition of the varnish films was a rapid test and it was applied to the largest selection of oil paints. Testing was carried out using a modified method historically used by varnish makers [4]. A solid varnish film immersed in water absorbs water and swells heavily (with a simultaneous decrease in firmness and increase in elasticity); this is a phase differentiation phenomenon that is called *imbibition* [4]. The swelling decreases when the liquid evaporates, but since the original state is not achieved (*hysteresis*), this leads to gradual deterioration of the solid film. The time taken for the film to turn opalescent or milky is used as an indicator of its water resistance, an important feature for anticorrosive paints. The test is carried out as follows: drops of liquid oil or varnish are spread on clean glass plates (microscope objective glasses) and dried for at least seven days. When the glass plates are submerged in distilled water, the time required to turn the film milky is measured. Typically, a duration of 60 h is used for the test, but in this study 24 h was used, as all films became milky in less than this time. The exposed glass plate was observed over black paper to achieve high contrast. The results are stated as sums of four replicates on solid unaged films.

### 3. Results and Discussion

#### 3.1. Liquid Samples

##### 3.1.1. Chemical and Physical Properties of Liquid Oils and Varnishes

First, as shown in Appendix A, the density or body differed for the varnishes, with the modern OH-L being the least bodied. Nevertheless, OH-L fell within the ISO 150:2006 and ISO 150:2018 standards for “boiled linseed oil” [22,23]. The refractive index was higher for the heat-bodied varnishes and highest for the tung oil T-L. The results from the cold test (and the insoluble impurities) confirmed that the turbidity was low in all samples, indicating high purity and low water content. The saponification value was about equal for all samples, and this also indicated that the purity was high for all the commercial oils. The alkaline impurities were slightly higher in OH-L but, on the other hand, its acid value was low. The low acid value is beneficial for use as a binder in aluminium-pigmented paints, since it does not react adversely with the amphoteric metallic pigments [24]. The highest acid value was observed for the stand oil WS-L, which was a result of the refinement process. In fact, it was observed that stand oil was able to etch the mild steel, since marks were seen visually in the application where the oil was applied with a pipette to the sheet before it was distributed over the surface. The water content was slightly higher for WHT-L, which is relevant because aluminium pigments are sensitive to water (risk of hydrogen formation) [24]. The iodine value indicates the proportion of unsaturated fatty acids and is often used for an estimation of the drying power. However, the iodine value alone does not reflect the influence of the catalysts or driers and their influence on the drying power [6]. For instance, the iodine value of a raw linseed oil could be the same as for a heat-treated oil with added driers (i.e., a varnish), as is also stated in the abovementioned standards. The presence of impurities, such as antioxidants, also influences the drying

power [25]. Also, the iodine value does not indicate the influence of the conjugated double bonds of tung oil [6]. The iodine value was significantly lower for the stand oils since a majority of the double bonds are consumed for conjugation and cyclic compound formation. The free fatty acid values and the peroxide values indicate the initiated decomposition and rancidification of the varnishes, and they were highest for the stand oils and the tung oil mixture. The peroxide value, in particular, measures the oxidation present (as hydroperoxides), suggesting that the degree of oxidation of the selected fresh oils differed. We expected the highest peroxide value for stand oil (WS-L) due to the processing methods and partial pre-polymerisation. Nevertheless, the heat-bodied varnish (WHT) had a value of 6: this may have been associated with the catalytic action of the manganese oxide present in the formulation, which accelerates the curing of oil.

### 3.1.2. FTIR

The FTIR spectra depicted in Figure 1 are characterised by the typical absorption peaks of fresh drying oils, and a summary of relevant bands in the FTIR spectra for each oil is provided in Table 2. Fresh oils show typical absorption spectra, with sharp and narrow bands ascribed to  $\nu$  C=O and only weak signal ascribed to  $\nu$ (O-H), suggesting that oxidation had not occurred. Moreover, well-defined bands in the  $\nu$  C-H region are visible for all oils. WT and WS can be clearly differentiated from the other oils on account of the strong absorption at  $990\text{ cm}^{-1}$  and  $964\text{ cm}^{-1}$ .

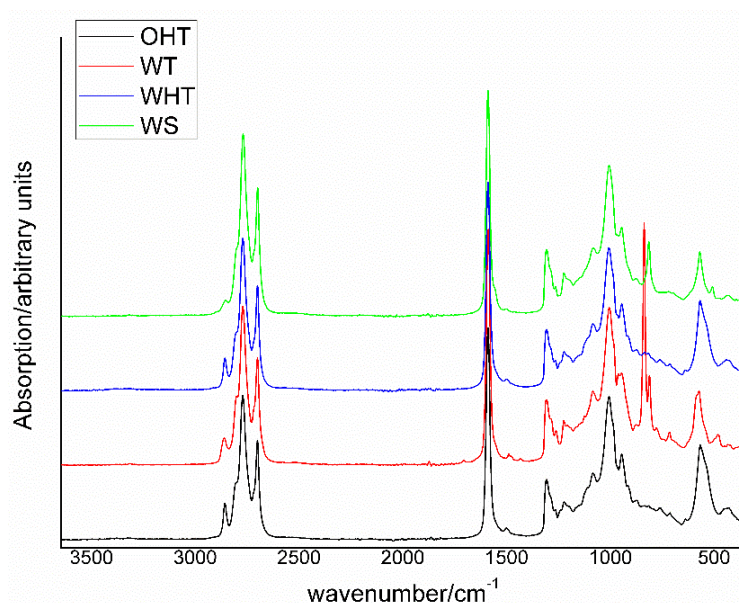


**Figure 1.** ATR-FTIR of oils prior to ageing. Spectra are shown normalised to the  $\nu$ C=O at  $1740\text{ cm}^{-1}$  and offset for clarity. Well-defined bands can be seen in the C-H stretching region. Stand oil and tung oil show strong bands at  $990\text{ cm}^{-1}$  and  $964\text{ cm}^{-1}$ .

### 3.1.3. GC-MS

The GC-MS analysis of fresh oils provided a full characterisation of the fatty acids contained in the selected commercial binders. This is important for manufactured binders since it is known that 20th and 21st century artists' oils and varnishes may contain different kinds of oils (drying, semi-drying and/or non-drying), a variety of additives (such as stabilisers, dispersion agents, etc.) and adulterations [15,27].

Appendix B lists all the compounds identified by GC-MS in the analysed samples.

As expected for fresh oils, the mono-, doubly and triply unsaturated fatty acids (oleic, linoleic and linolenic acids, respectively) were the most abundant compounds detected in the chromatograms in the case of linseed oils (OH-L, WHT-L and WS-L), together with glycerol (and glycerol derivatives). For the mixture containing tung oil (WT-L),

$\alpha$ -eleostearic acid (a conjugated linolenic acid the mass spectrum of which is shown in Figure 2a) was identified as the major compound. This triply unsaturated fatty acid is, indeed, the marker for tung oil [26].

**Table 2.** Summary of FTIR bands for liquid oils prior to ageing, with assignments based on [26].  $\nu$  = stretching,  $\delta$  = deformation,  $\omega$  = wagging,  $\Upsilon$  = out-of-plane deformation.

Assignment	Linseed Oils	OH-L	WHT-L	WS-L	Tung Oils	T-L
$\nu$ (O-H)			3067		3451	
	-/3340		3047			
$\nu$ (C-H) in C=C-H	3008/-	3010	3010		3012	3013
				3006		
$\nu$ (C-H)	2954 sh/overlapped	2956			2954	2953
$\nu$ (C-H)	2924	2924	2923	2922	2932/2927	2924
$\nu$ (C-H)	2852	2853	2853	2853		
$\nu$ (C=O)	1744/1740	1743	1742	1742	1745/1740	1741
$\nu$ (C=C)	1652/1634 sh	1654	1654	1656	1642	1642
			1587			1586
			1521			
$\delta$ (C-H) in methyl	1461/1462	1460	1460	1459	1464/1461	1459
$\delta$ (C-H) in methylene	1418/1416	1418	1418	1418	1416/1415	
$\delta$ (C-H) in methyl	1375	1376	1376	1376	1376/1377	1377
$\nu$ (C-O) in C-O-C in esters	1238/1240	1237	1238	1235	1238/1240	1237
$\nu$ (C-O) in C-O-C in esters	1163/1165	1160	1160	1159		1159
				1119		
$\nu$ (C-O) in C-O-C in esters	1099	1099	1098	1099	1100	1099
		1069	1069			
		1028	1029			
					992	990
		987	987		975	
$\omega$ (CH) in CH=CH wagging isolated trans	-/971	969	970	967	965	964
		914	914			
				872		
				852		
				807		
		866	867			
		791	792			
$\delta$ /CH <sub>2</sub> ) rocking	-/720	721	721	722	728	726

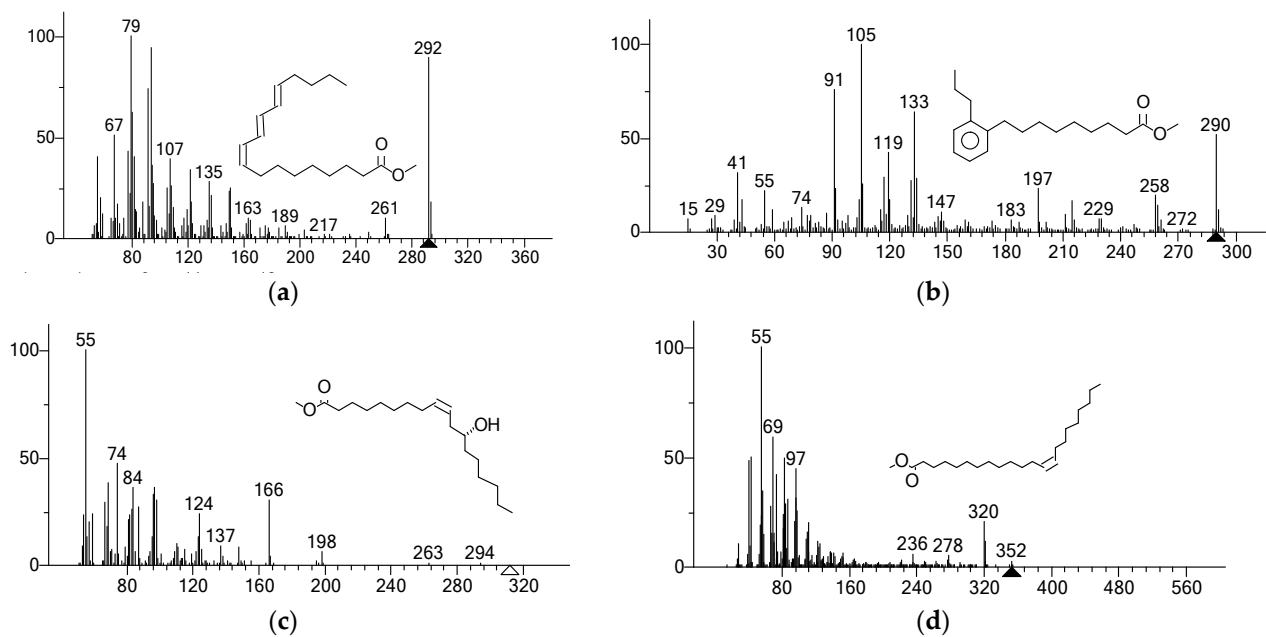


**Figure 2.** (a) Mass spectrum of  $\alpha$ -oleostearic acid (methyl ester), detected in WT-L; (b) mass spectrum of 9-(*o*-propylphenyl)-nonanoic acid methyl ester, identified in WS-L, WHT-L and WT-L; (c) mass spectrum of ricinoleic acid (methyl ester), identified in WHT-L; (d) mass spectrum of erucic acid (methyl ester), detected in WS-L.

In the stand oil varnish (WS-L), bicyclic compounds were detected (as methyl esters), such as 7-(*o*-pentylphenyl)-heptanoic acid and 9-(*o*-propylphenyl)-nonanoic acid (the mass spectrum of which is depicted in Figure 2b). These are cyclisation products due to the high temperature and anaerobic conditions of the oil processing method, which induce a partial pre-polymerisation, and they are considered specific markers for stand oils [28]. Nevertheless, these compounds were also identified in WHT-L (and then in WT-L, where 80% of the mixture was composed of WHT-L), meaning that the temperature reached in the oil processing (280 °C, as declared by the manufacturer) and the heating condition were enough to promote their formation. This finding actually explains the measurement of the highest peroxide value for WHT-L.

Comparing the GC-MS results obtained from the different fresh oils—and, in particular, the P/S (palmitic to stearic acid) ratios and the presence of uncommon fatty acids—it was possible to observe that:

- OH-L shows the typical fatty acid profile of linseed oil, corroborated by a P/S ratio of 1.7; all special fatty acids were found in this formulation;
- WHT-L, which, similarly to stand oil, was found to contain cyclic compounds, also contained castor oil, as indicated by the identification of its marker (i.e., ricinoleic acid—mass spectrum in Figure 2c). This non-drying oil can be found in modern commercial artist oil formulations as an adulterant in linseed oil or added for rheological purposes [29]. Castor oil is made into a drying oil by dehydration through the formation of an unsaturated hydroxy fatty acid [6]. In raw and blown form it serves as a plasticiser in coatings. In hydrated form, castor oil improves the elasticity, water resistance, alkali resistance and colour retention of paint, similar to tung oil. Its presence likely influenced the final P/S ratio of the mixture, which was 1.2. Indeed, castor oil's P/S ratio is generally around 1, while linseed oil has a P/S ratio ranging from 1.3 to 1.8 [30];
- WS-L contains a special monounsaturated fatty acid, namely erucic acid (mass spectrum in Figure 2d), which is considered as the biomarker for seeds of the *Brassicaceae* family, such as rapeseed. Rapeseed oil is a semi-drying oil that was introduced in the 20th century as a lubricant and/or as an adulterant in linseed oils [29,31]. Again,



- the presence of a mixture of different oils could have slightly modified the P/S ratio, which was 1.2;
- The mixture containing WHT-L and tung oil did not contain any additional oils and presented a P/S ratio of 1.2.

### 3.2. Solid Samples

#### 3.2.1. Artificial Ageing

Artificial ageing occurred over a total of 27 h. The first aged sample (A1) of each variant was removed after 17 h and the second (A2) after 27 h. All samples showed rust-coloured areas, most probably indicating inhomogeneities in the solid films (Figure 3). The relative degree of rusty surfaces was used as an indicator of moisture penetration and ageing, and this was assessed visually. Incident daylight and UV light was also used to estimate if there were areas without film. The samples for further analysis were removed from areas with no or very little rust colour, and the degree of rust colour was determined.

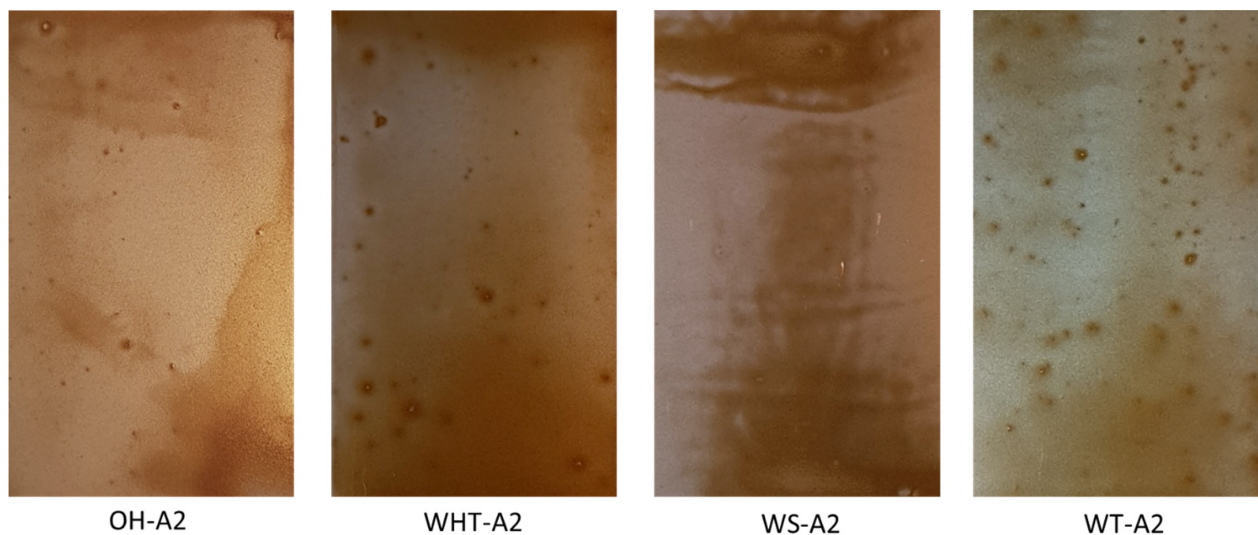


**Figure 3.** The appearance of the aged varnishes (A2). There is no colour correction in the photographs, they are only provided to give a hint of how the films aged. It was observed that water had penetrated the films and reached the metal, resulting in corrosion in localised areas and spots.

#### 3.2.2. Water Immersion Test

Solid films (dried for four weeks in lab conditions) were tested to evaluate their capacity to absorb water. The results are reported in Figure 4 and Table 3 and show that the modern linseed oil varnish (OH-0), as well as both the manganese oxide varnishes (WHT-0, P-0), became milky after a very short time when immersed in distilled water; indeed, the appearance of the solid films began to change after only 1.5 h. In contrast, when 20 wt% tung oil was added to these varnishes (WT-0), the water absorption decreased significantly and was comparable to the stand oil (WS-0) and litharge varnish: their appearance was almost unaffected after more than 24 h. The results indicated that fresh films based on stand oils, any varnish with the addition of 20 wt% tung oil, and litharge varnish had high resistance to water exposure in immersion tests. They also indicated that the good performance of OH as binder in aged replica armour paint, as previously reported [2], is a result of the lamellar pigments' ability to delay the deterioration of the organic binder.

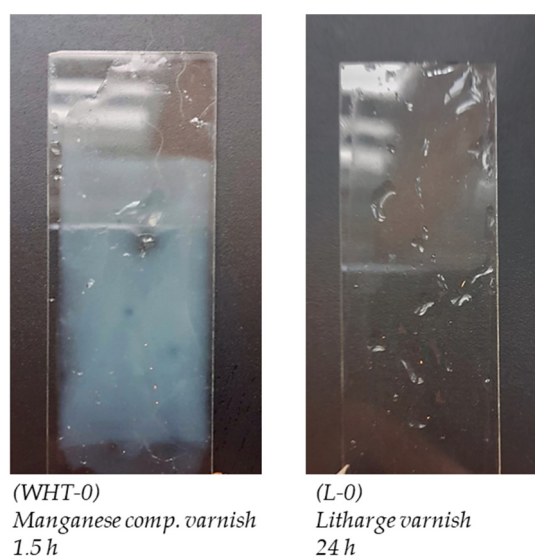


**Figure 4.** An example of low and high performance at the water immersion tests. On left: the WHT turns milky within 1.5 h, while the L-S is almost unaffected after 24 h. There is remaining water on the glass plates.

**Table 3.** The effect of water immersion on the appearance of solid varnish films applied on glass plates.

	OH-0	WHT-0	WS-0	WT-0	OHT-0	L-0	P-0	MB-0
Milky time	1.5 h	1.5 h	>24 h	>24 h	>24 h	>24 h	1.5 h	~16 h
Comments	White	White	*	*	*	*	White	Somewhat frosty appearance

\* Almost unaffected.

### 3.2.3. FTIR

The FTIR spectra of reference solid oil films prior to artificial aging revealed differences between the oils in the shapes of the C-H stretching bands and the shapes and positions of the  $\nu$  C=O, as well as the bands mentioned above for undried oils. Spectra recorded at all stages of accelerated ageing from the solid films (cured and aged) can be seen in Figures 5 and 6. The curing time (4 weeks) was sufficient to observe small changes in the FTIR spectra in comparison to the fresh liquid oils, as also reported in the literature [32,33]. The band at approximately  $3010\text{ cm}^{-1}$  related to  $\nu$ (C-H) in C=C-H is not visible for the solid oil films, suggesting partial oxidation of unsaturated bonds. In addition, the narrow band at approximately  $1742\text{ cm}^{-1}$  in liquids broadens and there is a loss in the definition of bands in the fingerprint region—all indications of the formation of new molecules with the onset of oxidation reactions prior to artificial ageing.

Artificial ageing causes significant changes in absorption that reflect bulk molecular changes. Generally, loss of definition of bands in the fingerprint region occurred following 64 kJ exposure, confirming the rapid chemical changes following the oxidation of the oils. The spectra from WT and OH are similar, as are those from WHT and WS films. Broadening of the carbonyl absorption is centred at approximately  $1740\text{ cm}^{-1}$  and changes in the shape of the band with a shoulder at  $1710\text{ cm}^{-1}$  reflect oxidation reactions and the formation of secondary oxidation products, including aldehydes [32]. Only slight modifications can be observed in the WHT, which are associated with a broadening of the C=O band, and there is a loss of absorption at  $968\text{ cm}^{-1}$ , ascribed to  $\omega$  (CH) in CH=CH wagging, which is in agreement with the findings from [26] for tung oils and indicated with a + in Figures 5 and 6. For the WS and OH, there is a significant increase in the absorption at  $1550\text{ cm}^{-1}$  ascribed to  $\nu_{as}$  and  $\nu_a$  of COO<sup>-</sup>, which can be attributed to the formation of metal carboxylates (resulting from the presence of metal oxide driers in the formulation).

Additional changes in the shape of the  $\nu$  OH can be seen with the growth of bands at  $1550\text{ cm}^{-1}$ , as has been reported in metal carboxylate formation. An increase in absorption at  $1425\text{ cm}^{-1}$  can be attributed to the oxidation of double bonds and the formation of  $\nu(\text{C-O})$  [34].

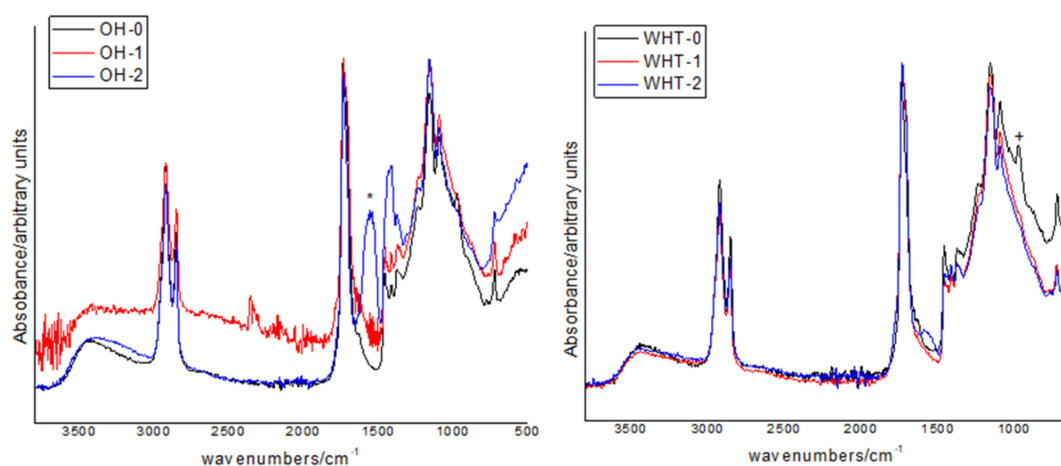


**Figure 5.** ATR-FTIR of solid films of paint binders OH and WHT at three different stages: prior to artificial ageing (0) and following exposure to 64 kJ hours (1) and 97 kJ (2). Changes in spectra occurred for all oils between stages 0 and 1 with the loss of definition of bands in the fingerprint region, including the band at  $968\text{ cm}^{-1}$  (+). Spectral changes between 1 and 2 can be ascribed to the formation of metal carboxylates (due to the driers present), with bands that appear at  $1550\text{ cm}^{-1}$  (\*), which was strongest in OH. Spectra are shown normalised to the  $\nu\text{C=O}$  at  $1740\text{ cm}^{-1}$ .

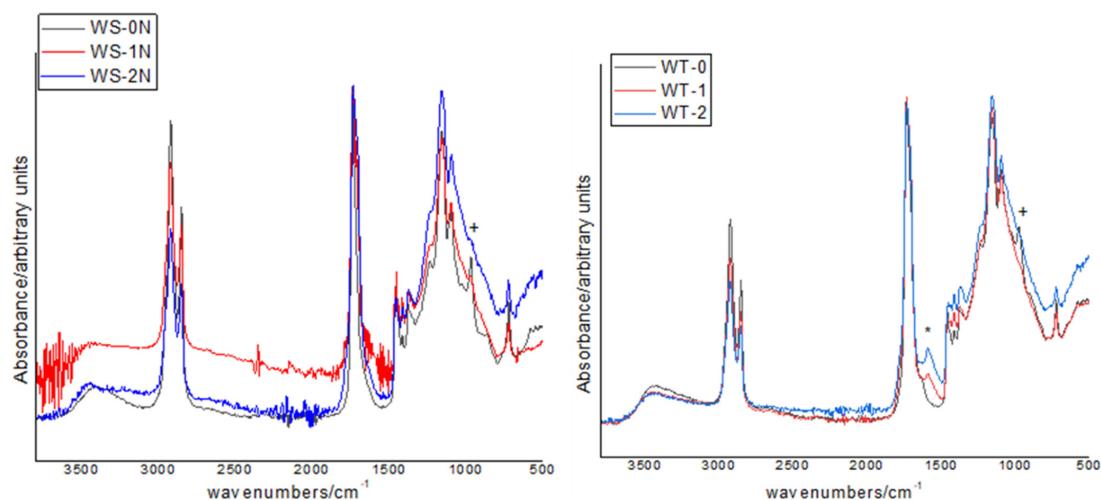


**Figure 6.** ATR-FTIR of solid films of paint binders WS and WT at three different stages: prior to artificial ageing (0) and following exposure to 64 kJ hours (1) and 97 kJ (2). Changes occurred for all oils between stages 0 and 1 with the loss of definition of bands in the fingerprint region, including the band at  $968\text{ cm}^{-1}$  (+). Changes between 1 and 2 can be seen, with weaker formation of carboxylates at  $1550\text{ cm}^{-1}$  (\*) in WT in comparison to OH (Figure 5). Spectra are shown normalized to the  $\nu\text{C=O}$  at  $1740\text{ cm}^{-1}$ .

### 3.2.4. GC-MS

GC-MS analysis allowed us to determine the fatty acid profiles of the unaged/aged solid samples. The obtained results are summarised in the graph in Figure 7, which reports the percentages of fatty acids (in weight), and in Table 4, which lists the most significant molar ratios among the selected fatty acids, together with fresh oils.

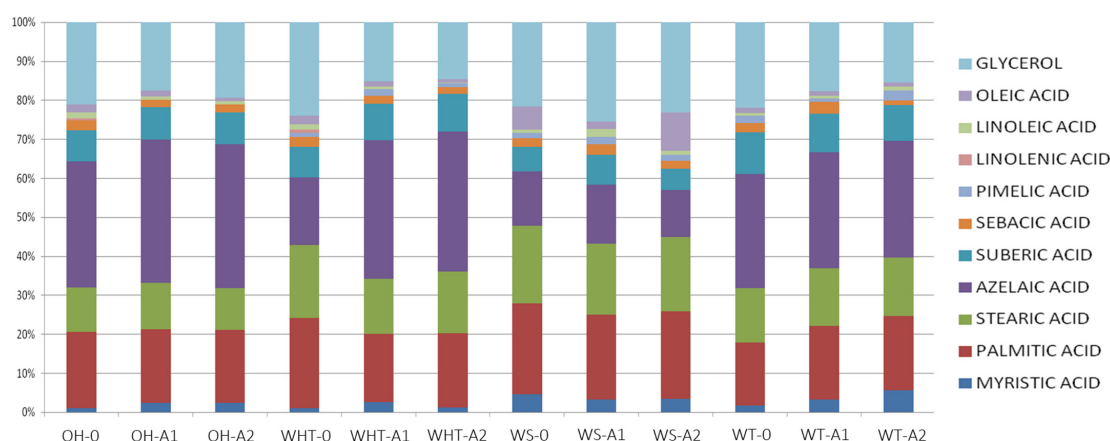


**Figure 7.** Graph illustrating the GC-MS results expressed in % weight of fatty acids and glycerol detected in unaged and aged solid samples.

**Table 4.** The molar ratios for the samples were calculated using GC-MS. Samples were from films prior to exposure (S) and following 64 kJ (A1) and 97 kJ (A2).

Molar Ratios	OH			WHT			WS			WT		
	OH-0	OH-A1	OH-A2	WHT-0	WHT-A1	WHT-A2	WS-0	WS-A1	WS-A2	WT-0	WT-A1	WT-A2
P/S	1.73	1.70	1.73	1.24	1.24	1.20	1.17	1.19	1.18	1.15	1.26	1.24
A/P	1.64	1.90	1.97	0.76	2.03	1.50	0.60	0.70	0.54	1.82	1.60	1.62
D/P	2.18	2.47	2.52	1.21	2.67	1.92	0.97	1.18	0.87	2.63	2.30	2.26
O/S	0.17	0.12	0.08	0.12	0.09	0.05	0.30	0.10	0.52	0.09	0.08	0.07
%D	42.86	47.03	47.30	28.85	48.63	47.33	23.82	27.46	21.09	44.26	43.74	43.05

Generally, the chromatograms exhibit all the characteristic fatty acids (as methyl esters) occurring in cured drying oils: short-chain fatty acids, dicarboxylic acids (pimelic, suberic, azelaic and sebacic acids), saturated long-chain fatty acids (myristic, palmitic, stearic, arachidic and behenic acids) and (traces of) unsaturated fatty acids. Several peaks related to glycerol derivatives were detected as well. The numerous and abundant oxidised octadecanoic (oxo-, hydroxy- and methoxy-octadecanoic) acids were produced by the oxidative scission of unsaturated fatty acids.

Dicarboxylic acids, such as azelaic, suberic and sebacic acids, are typical tertiary oxidation compounds from unsaturated fatty acids: they are the main oxidative degradation products and are formed as a consequence of fragmentations of triglycerides occurring in the cross-linked network. The D%, A/P and D/P molar ratios can provide an important overview of how different oils behave after 4 weeks of auto-oxidation. WT-S had the largest values (A/P = 1.82, D/P = 2.63, %D = 44.26), followed by OH-S (A/P = 1.64, D/P = 2.18, %D = 42.86).

The proportion of dicarboxylic acids in the unaged solid films was lower for WHT-S and WS-S (possibly also because of the presence of semi-drying and non-drying portions of the lipidic binders).

For the unaged solid films, since they were relatively young (4 weeks) and did not contain any pigment, the doubly and triply unsaturated fatty acids were still detectable (see Figures 5 and 6); nevertheless, their concentrations were much lower compared to the liquid binder (on average, more than 50–60% of the total fatty acids) after autoxidation took place (as evidenced by FTIR spectra). The high amount of oleic acid (see the O/S ratios in Table 4) can be explainable by the relatively young age of the films and by the minor autoxidation reaction compared to doubly and triply unsaturated acids [35,36]. In the case of the tung oil mixture WT-S, it was not possible to detect  $\alpha$ -eleostearic acid: this triply unsaturated fatty acid is very rapidly subjected to oxidation, as stated in [26].

For the paint films subjected to 97 kJ, the GC/MS results highlighted the effect of photo-oxidation. Thus, as expected, a general decrease in unsaturations, (oleic, linoleic and linolenic acids for linseed-based oils and  $\alpha$ -eleostearic acid in the case of tung oil) and a general increase in dicarboxylic acids (D/P ratios and D%), in particular azelaic acid (A/P ratios), was registered. An example of changes in the chromatograms for the OH film series is illustrated in Figure 8.

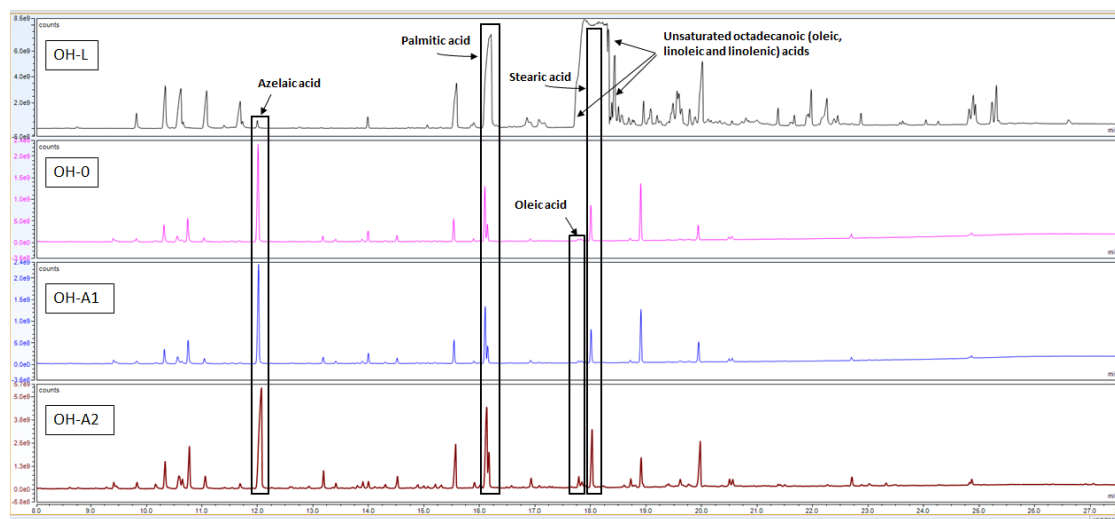


**Figure 8.** Total ion current (TIC) chromatograms after derivatisation and GC-MS analysis of OH: L, liquid; 0, solid reference; A1, aged 1 (64 kJ); A2, aged 2 (97 kJ). It is possible to observe the decrease in unsaturated fatty acids (oleic, linoleic and linolenic) with ageing and the increase in azelaic acid as the main oxidation product during ageing. Despite the incomplete separation of the peaks at the chromatographic level, the identification of the different unsaturated fatty acids (oleic, linoleic and linolenic) was possible thanks to the detection of the typical  $m/z$  spectra through the mass spectrometer. For further details, see the table in Appendix B.

This study used relatively short accelerated ageing conditions, following ISO 16474:2013, to test the performances of refined and bodied linseed oils and tung oil as binders in armour paints. The considered ageing conditions represented a heavily simplified model of natural conditions and conditions usually employed for the study of fine art materials. In nature, the response to atmospheric exposure is dependent on geographical conditions as well as how the paint is applied and used on the substrate. It is recognized and confirmed by the results above that organic paint binders follow very complex chemical reactions, leading to different physical and mechanical characteristics, depending on how the binders are produced and used and how they age. The search for tools to understand and control these patterns is an extensive task. It is complicated by additions of other (semi- and non-drying) vegetable oils to commercially sold binders, as well as different paint ingredients and formulations. Chemical and physical data (such as the iodine value, refractive index, colour, etc.) represent important properties, which are used in industry to control the reproducibility of different refining processes and outcomes and to recommend the oils and varnishes for different possible uses. However, the complex chemistry leading to film formation and oxidation cannot be explained simply with reference to these standard data. Indeed, the behaviour of the oils, their reactions with pigments and other paint ingredients, and the ageing characteristics of the oils, varnishes and paints are highly complex and require more sophisticated molecular analysis, as shown with GC-MS.

The water immersion test is an example of a simple and useful quality assessment method, originally from the varnish and paint-making industry, that can be used in the search for suitable and high-quality fat varnishes for new paint formulations based on older knowledge. For investigations of anticorrosive coating, electrochemical impedance spectroscopy (EIS) has often been cited for its use in the examination of the influence of pigments and binders on barrier properties [37,38]. EIS is suitable for industrial coatings

(such as powder spraying), and the method involves the use of different (often quite aggressive) electrolytes—conditions that are hard to correlate to the *in situ* anticorrosive painting of ferrous heritage, which has different environmental conditions. The same is valid for methods that measure the levels of macro- and micro-defects that determine the water vapour transmission rate, such as ellipsometric porosimetry (EP).

#### 4. Conclusions

Analysis of binders used in armour paints revealed important differences between commercial oils, many of which contained additives that were only detectable with GC-MS. FTIR analysis of films revealed changes in the chemical groups at the surface and was complemented by GC-MS bulk analysis. GC-MS provided other detailed information about the lipidic composition of the binders. Still, it was difficult to univocally correlate the fatty acid profiles and the different fatty acid ratios to the environmental responses of films to ageing. These methods in combination revealed similarities between the four organic binders tested, such as the presence of saturated and unsaturated mono/dicarboxylic acids and oxidative scission reactions. Differences could also be observed, such as the presence of cyclic compounds in stand oil and the high-temperature-treated varnish, biomarkers for additions of other types of vegetable oils in two of the samples and varying fatty acid ratios.

Although FTIR and GC-MS did not reveal any direct information about the colloidal state of the binders, the presence and the amount of unsaturated fatty acids (oleic, linoleic and linolenic in linseed oil and  $\alpha$ -eleostearic in tung oil) detected by GC-MS and the observations of the O/S ratios in fresh oils and solid films may provide important indications about the reactivity (and “maturity”) of the oil or varnish. The water immersion test easily reveals phase differentiation in solid films. This occurred quite rapidly, after only 1.5 h for the modern linseed oil varnish as well as for the pyrolusite high-temperature varnishes. In fact, the same type of relationship could also be observed for these varnishes in the accelerated ageing (OH and WHT behaved in similar ways). Higher or equal resistance to polar solvent absorption and imbibition was reached for the litharge varnish, the stand oil and all varnishes with tung oil additions. During accelerated ageing, this tendency enabled the moisture to reach the steel surface, which started to corrode. If this process had been left to proceed, the films would most probably have been ruined by the volume expansion of the corrosion products and not by the deterioration of the films through the impact of oxidation, hydrolysis and other degenerative processes.

Future research should consider the longer-term reactions of binders mixed with different pigments in natural and controlled aging conditions, using physical as well as chemical testing. Additional monitoring of the water-soluble components of the different films would likely reveal some of the chemical reactions that occur with ageing.

**Author Contributions:** Conceptualization, F.C.I. and A.K.; investigation, F.C.I. and A.K.; methodology, F.C.I., A.K. and A.N.; formal analysis, F.C.I., A.K. and A.N.; visualization, F.C.I., A.K. and A.N.; writing—review and editing, A.K. and A.N.; project administration, A.K.; writing—original draft, review and editing, A.K.; supervision, A.N. All authors have read and agreed to the published version of the manuscript.

**Funding:** This research received no external funding.

**Institutional Review Board Statement:** This study involves no humans or animals. The study was conducted according to the guidelines of the Declaration.

**Informed Consent Statement:** Not applicable.

**Data Availability Statement:** Data from this study are available at request from the authors.

**Acknowledgments:** Francesca C. Izzo would like to thank the “Patto per lo Sviluppo della Città di Venezia” (Municipality of Venice) for the support in the research.

**Conflicts of Interest:** The authors declare no conflict of interest.

## Appendix A. Chemical and Physical Properties of the Paint Binders

	Measured Property/Characteristic				Results on Commercial Binders			
	Methodological Details				OH-L	WHT-L	WS-L	T-L
	Method	Unit/at	At	Uncert., %				
Density	Electronic	g/cm <sup>3</sup>	20 °C	-	0.9339	0.9370	0.9575	0.9391
Refractive index	Automatic	-	20 °C	±0.01	1.4826	1.4823	1.4907	1.5194
			60 °C	±0.01	1.4682	1.4679	1.4763	>1.5000
Cold test	AAK method	-	6 h	-	2	2	2	2
Insoluble impurities	AOCS Ca 3a-46	%		20	<0.01	0.01	<0.01	<0.01
Alkaline impurities	EP 2.4.19	ml		-	0.15	<0.10	<0.10	<0.10
Water content	AOCS CA 2E-84	%		±15	0.06	0.1	0.03	0.04
Iodine value	AOCS Cd 1c-85 + ISO 3961	mg iodine/100 g		-	196	177	112	161
Saponification value	IUPAC 2.202	mg KOH/g		±2	188	191	192	192
Free fatty acids	IUPAC 2.201 (m)	-	282	±3	0.94	1.7	3.1	1.7
Acid value	IUPAC 2.201 (m)	mg KOH/g		±3	1.87	3.41	6.24	3.3
Peroxide value	AOCS Cd 8-53	meq/kg		±15	2.6	6	3.3	5.6
			Yellow	±25	130.0	140.0	40.0	60.0
Colour (Lovibond)	AOCS Cc 13j-97		Red		20.0	14.0	3.0	7.0
			Blue		0.0	0.0	0.0	0.0
			Total		330.0	280.0	70.0	130.0

### References Appendix A

- European Pharmacopeia Commission. *Alkaline impurities in fatty oils. Methods of analysis EP 2.4.19; EU*; European Pharmacopeia Commission: Strasbourg, Germany, **2005**.
- International Organization for Standardization. (2018). *Animal and vegetable fats and oils. Determination of iodine value. (ISO 3961:2018)*; International Organization for Standardization: Geneva, Switzerland, **2018**
- IUPAC (1992). *Determination of the saponification value (S.V). Standard Methods for the Analysis of Oils, Fats and Derivatives. IUPAC 2.202:1992*; Oxford, United Kingdom: International Union of Pure and Applied Chemistry Commission on Oils, Fats and Derivatives, **1992**.
- IUPAC (1992). *Determination of the acidity of lecithins. Standard Methods for the Analysis of Oils, Fats and Derivatives. IUPAC 2.201/(5.201)*; Oxford, United Kingdom: International Union of Pure and Applied Chemistry Commission on Oils, Fats and Derivatives, **1992**.
- IUPAC (1992). *Capillary column gas—liquid chromatography of fatty acid methyl esters. Standard Methods for the Analysis of Oils, Fats and Derivatives. IUPAC 2.304:1992*; Oxford, United Kingdom: International Union of Pure and Applied Chemistry Commission on Oils, Fats and Derivatives, **1992**.
- AOCS (2017). *Moisture. Karl Fischer Method. AOCS Official Method Ca 2e-84, revised 2017*. Urbana, USA: The American Oil Chemists' Society, **2017**.
- AOCS (2017). *Calculated Iodine Value. AOCS Official Method AOCS Cd 1c-85, revised 2017*; Urbana, USA: The American Oil Chemists' Society, **2017**.
- AOCS (2003). *Peroxide Value—Acetic Acid-Chloroform Method. AOCS Official Method AOCS Cd 8-53 (1953/revised 2003)*; Urbana, USA: The American Oil Chemists' Society, **2003**.
- AOCS (2017). *Insoluble Impurities in Fats and Oil. AOCS Official Method AOCS Ca 3a-46, revised 2017*; Urbana, USA: The American Oil Chemists' Society, **2017**.
- AOCS (2017). *Color of Fats and Oils, Automated Method. AOCS Official Method AOCS Cc 13j-97, revised 2017*; Urbana, USA: The American Oil Chemists' Society, **2017**.





Table A1. Cont.

RT (min)	Identified Compound	OH				WHT				WS				WT			
		OH-L	OH-0	OH-1	OH-2	WHT-L	WHT-0	WHT-1	WHT-2	WS-L	WS-0	WS-1	WS-2	WT-L	WT-0	WT-1	WT-2
19.210	Alpha-eleostearic acid methyl ester													✓			
19.570	Ricinoleic acid methyl ester					✓	✓	✓	✓								
19.624	Octadecanoic acid, 10-oxo-, methyl ester		✓	✓	✓		✓	✓	✓		✓	✓	✓		✓	✓	✓
19.767	Arachidic acid methyl ester		✓	✓	✓		✓	✓	✓		✓	✓	✓		✓	✓	✓
19.803	7-(o-pentylphenyl)-heptanoic acid methyl ester					✓					✓				✓		
19.883	9-(o-propylphenyl)-nonanoic acid methyl ester					✓					✓				✓		
19.944	Glycerol (main)	✓	✓	✓	✓	✓	✓	✓	✓	✓	✓	✓	✓		✓	✓	✓
21.196	Erucid acid methyl ester									✓	✓	✓	✓				
21.386	Behenic acid, methyl ester		✓	✓	✓		✓	✓	✓		✓	✓	✓		✓	✓	✓
22.712	Octadecanoic acid, 9,10-epoxy		✓	✓	✓		✓	✓	✓		✓	✓	✓		✓	✓	✓
22.885	Tetracosanoic acid, methyl ester		✓	✓	✓		✓	✓	✓		✓	✓	✓		✓	✓	✓
24.287	Hexacosanoic acid, methyl ester		✓	✓	✓		✓	✓	✓		✓	✓	✓		✓	✓	✓
24.817	β-Monolinolein	✓				✓					✓						
24.875	Octadecanoic acid, 9,10-oxo-, methyl ester		✓	✓	✓		✓	✓	✓		✓	✓	✓		✓	✓	✓
24.889	Linolenic acid 1,3-dimethoxypropan-2-yl ester	✓				✓					✓						
24.930	Linolenic acid, 2-hydroxy-1-(hydroxymethyl)ethyl ester (Z,Z,Z)-	✓				✓					✓						
25.561	Sitosterol										✓						

## References

1. Källbom, A. The Concept of Anticorrosive Aluminium-Pigmented Armour Paint, for Sustainable Maintenance of Ferrous Heritage. *Int. J. Archit. Herit.* **2021**, *14*, 1–19. [\[CrossRef\]](#)
2. Källbom, A.; Izzo, F.; Nevin, A. Multi-analytical assessment of Armour Paints: The Ageing Characteristics of Historic Drying Oil Varnish Paints for Protection of Steel and Iron Surfaces in Sweden. *Heritage* **2021**, *4*, 63. [\[CrossRef\]](#)
3. Standeven, H. *House Paints, 1900–1960: History and Use*; Getty Conservation Institute: Los Angeles, CA, USA, 2011.
4. Magnusson, K.H. Linoljans framställning och förädling. [The Manufacturing and Refinement of Linseed Oil]. In *Tekniska Samfundets i Göteborg. Avdelningen för Kemi och Fysik. 1914–1939*; Göteborgslitografen: Göteborg, Sweden, 1939; pp. 253–266.
5. Sabin, A.H. *Industrial and Artistic Technology of Paint and Varnish*, 3rd ed.; John Wiley & Sons: New York, NY, USA, 1927.
6. Singer, E. *Fundamentals of Paints, Varnish and Lacquer Technology*; The American Paint Journal Company: Washington, DC, USA, 1957.
7. Lazzari, M.; Chiantore, O. Drying and Oxidative Degradation of Linseed Oil. *Polym. Degrad. Stab.* **1999**, *65*, 303–313. [\[CrossRef\]](#)
8. Scalarone, D.; Lazzari, M.; Chiantore, O. Thermally Assisted Hydrolysis and Methylation-pyrolysis-gas chromatography/mass spectrometry of Light-aged Linseed Oil. *J. Anal. Appl. Pyrolysis* **2001**, *58–59*, 503–512. [\[CrossRef\]](#)
9. Stern, E. Farbenbindemittel, Farbkörper und Anstrichstoffe. In *Kolloidchemische Technologie*; Ein Handbuch Kolloidchemischer Betrachtungsweise in der Chemischen Industrie und Technik; Lesegang, R.E., Ed.; Springer: Berlin, Germany, 1932.
10. Auer, L. Colloidal Chemistry of Drying Oils. *Ind. Eng. Chem.* **1938**, *30*, 466–472. [\[CrossRef\]](#)
11. Dietemann, P.; Neugebauer, W.; Lutz, L.; Beil, C.; Fiedler, I.; Baumer, U. A Colloidal Description of Tempera and Oil Paints, based on a Case Study of Arnold Böcklin's Painting Villa am Meer (1865). *e-PRESERVATIONSCIENCE* **2014**, *11*, 29–46.
12. Berg, J. *Introduction to Interfaces and Colloids*; World Scientific Publishing Company: Singapore, 2009.
13. International Organization for Standardization. *ISO 16474-2:2013. Paints and Varnishes—Methods of Exposure to Laboratory Light Sources. Part 2: Xenon-Arc Lamps*; International Organization for Standardization: Geneva, Switzerland, 2013.
14. Fuster-López, L.; Izzo, F.C.; Piovesan, M.; Sporni, L.; Zendri, E. Study of the chemical composition and the mechanical behaviour of 20th century commercial artists' oil paints containing manganese-based pigments. *Microchem. J.* **2016**, *124*, 962–973. [\[CrossRef\]](#)
15. Izzo, F.C.; Zanin, C.; van Keulen, H.; Da Roit, C. From pigments to paints: Studying original materials from the atelier of the artist Mariano Fortuny y Madrazo. *Int. J. Conserv. Sci.* **2017**, *8*, 547–564.
16. Caravá, S.; García, C.R.; de Agredos-Pascual, M.L.V.; Mascarós, S.M.; Izzo, F. Investigation of modern oil paints through a physico-chemical integrated approach. Emblematic cases from Valencia, Spain. *Spectrochim. Acta. Part A Mol. Biomol. Spectrosc.* **2020**, *240*, 118633. [\[CrossRef\]](#)
17. Fuster-López, L.; Izzo, F.; Damato, V.; Yusà-Marco, D.; Zendri, E. An insight into the mechanical properties of selected commercial oil and alkyd paint films containing cobalt blue. *J. Cult. Herit.* **2019**, *35*, 225–234. [\[CrossRef\]](#)
18. Fuster-López, L.; Izzo, F.C.; Andersen, C.K.; Murray, A.; Vila, A.; Picollo, M.; Stefani, L.; Jiménez, R.; Aguado-Guardiola, E. Picasso's 1917 paint materials and their influence on the condition of four paintings. *SN Appl. Sci.* **2020**, *2*, 1–14. [\[CrossRef\]](#)
19. Hermans, J.J.; Keune, K.; Van Loon, A.; Iedema, P.D. Toward a complete molecular model for the formation of metal soaps in oil paints. In *Metal Soaps in Art*; Springer: Cham, Switzerland, 2019.
20. Izzo, F. 20th Century Artists' Oil Paints: A Chemical-Physical Survey. Ph.D. Thesis, University "Ca' Foscari", Venice, Italy, 2011.
21. Izzo, F.C.; van den Berg, K.J.; van Keulen, H.; Ferriani, B.; Zendri, E. Modern Oil Paints—Formulations, Organic Additives and Degradation: Some Case Studies. In *Issues in Contemporary Oil Paint*; van den Berg, K.J., Burnstock, A., de Keijzer, M., Krueger, J., Learner, T., Tagle, A., Heydenreich, d., Eds.; Springer: Cham, Switzerland, 2014.
22. International Organization for Standardization. *Raw, Refined and Boiled Linseed Oil for Paints and Varnishes—Specifications and Methods of Test. ISO 150:2006*; ISO International Organization for Standardization: Geneva, Switzerland, 2006.
23. International Organization for Standardization. *Raw, Refined and Boiled Linseed Oil for Paints and Varnishes—Specifications and Methods of Test. ISO 150:2018*; ISO International Organization for Standardization: Geneva, Switzerland, 2018.
24. Edwards, J.D. *Aluminum Paint and Powders*, 1st ed.; Reinhold Publishing Corporation: New York, NY, USA, 1936.
25. Gupta, M. *Practical Guide to Vegetable Oil Processing*, 2nd ed.; Elsevier Science: Amsterdam, The Netherlands, 2017.
26. Schönemann, A.; Edwards, H. Raman and FTIR microspectroscopic study of the alteration of Chinese tung oil and related drying oils during ageing. *Anal. Bioanal. Chem.* **2011**, *400*, 1173–1180. [\[CrossRef\]](#)
27. Learner, T.; Getty Conservation Institute. *Analysis of Modern Paints*; Getty Conservation Institute: Los Angeles, CA, USA, 2004.
28. Sebedio, J.L.; Grandgirard, A. Cyclic fatty acids: Natural sources, formation during heat treatment, synthesis and biological properties. *Prog. Lipid Res.* **1989**, *28*, 303–336. [\[CrossRef\]](#)
29. Izzo, F.C.; Ferriani, B.; Van Den Berg, K.J.; Van Keulen, H.; Zendri, E. 20th Century Artists' Oil Paints: The Case of the Olii by Lucio Fontana. *J. Cult. Herit.* **2014**, *15*, 557–563. [\[CrossRef\]](#)
30. Colombini, M.P.; Modugno, F. (Eds.) *Organic Mass Spectrometry in Art and Archaeology*; John Wiley & Sons Inc.: Hoboken, NJ, USA, 2009.
31. Van Keulen, H. Slow-drying oil additives in modern oil paints, and application in conservation treatments. An analytical study in technical historical perspective. In *ICOM Committee for Conservation 17th Triennial Meeting Melbourne Australia 19–23 September 2014*; ICOM Committee for Conservation: Melbourne, Australia, 2014.

32. Brambilla, L.; Riedo, C.; Baraldi, C.; Nevin, A.; Gamberini, M.C.; D'Andrea, C.; Chiantore, O.; Goidanich, S.; Toniolo, L. Characterization of fresh and aged natural ingredients used in historical ointments by molecular spectroscopic techniques: IR, Raman and fluorescence. *Anal. Bioanal. Chem.* **2011**, *401*, 1827. [[CrossRef](#)] [[PubMed](#)]
33. Van der Weerd, J.; van Loon, A.; Boon, J.J. FTIR Studies of the Effects of Pigments on the Aging of Oil. *Stud. Conserv.* **2005**, *50*, 3–22. [[CrossRef](#)]
34. Izzo, F.C.; Kratter, M.; Nevin, A.; Zendri, E. A Critical Review on the Analysis of Metal Soaps in Oil Paintings. *ChemistryOpen* **2021**, *10*, 904–921. [[CrossRef](#)]
35. Wexler, H. Polymerization of drying oils. *Chem. Rev.* **1964**, *64*, 591–611. [[CrossRef](#)]
36. Van den Berg, J.D.; Van den Berg, K.J.; Boon, J.J. Identification of non-cross-linked compounds in methanolic extracts of cured and aged linseed oil-based paint films using gas chromatography–mass spectrometry. *J. Chromatogr. A* **2002**, *950*, 195–211. [[CrossRef](#)]
37. Araujo, W.S.; Margarit, I.C.P.; Mattos, O.R.; Fragata, F.L.; de Lima-Neto, P. Corrosion Aspects of Alkyd Paints Modified with Linseed and Soy Oils. *Electrochim. Acta* **2010**, *55*, 6204–6211. [[CrossRef](#)]
38. Perrotta, A.; García, S.J.; Creatore, M. Ellipsometric Porosimetry and Electrochemical Impedance Spectroscopy Characterization for Moisture Permeation Barrier Layers. *Plasma Process. Polym.* **2015**, *12*, 968–979. [[CrossRef](#)]